Preparation of sharp polycrystalline tungsten tips for scanning tunneling microscopy imaging

R. Zhang, and D. G. Ivey

Citation: Journal of Vacuum Science & Technology B: Microelectronics and Nanometer Structures Processing, Measurement, and Phenomena **14**, 1 (1996); doi: 10.1116/1.589029

View online: https://doi.org/10.1116/1.589029

View Table of Contents: http://avs.scitation.org/toc/jvn/14/1

Published by the American Institute of Physics

Preparation of sharp polycrystalline tungsten tips for scanning tunneling microscopy imaging

R. Zhang and D. G. Ivey
Department of Mining, Metallurgical, and Petroleum Engineering, University of Alberta, Edmonton, Alberta, Canada T6G 2G6

(Received 13 March 1995; accepted 27 October 1995)

The fabrication of scanning tunneling microscopy (STM) tips by dc downward electrochemical polishing and ion milling has been investigated. The influence of parameters, such as voltage, immersion depth, cutoff time, and solution concentration, on the shape and sharpness of electropolished W tips are presented. Both electropolished and ion milled tips, which were characterized by transmission electron microscopy (TEM), were tested on Au films deposited on ⟨100⟩ oriented Si. The effects of tip radius on STM images are discussed thoroughly, and the results are also compared to atomic force microscopy (AFM) and TEM images. © *1996 American Vacuum Society.*

I. INTRODUCTION

Ever since scanning tunneling microscopy (STM) was developed by Binnig *et al.*,[1–3] there has been considerable interest in making sharp metal tips for high resolution imaging. Tip shape and sharpness are the two most important parameters in imaging surfaces, particularly those with significant topography. STM images invariably include contributions from specimen structure and tip geometry. Thus, the study of the tip geometry is indispensable in distinguishing between the apparent and the true structure or to establish the relationship among the tip geometry, true surface structure, and STM image.

The various tip preparation procedures can be divided into two main categories: (i) mechanical or (ii) physicochemical.[4] Mechanical procedures include cutting,[5] machining,[1] and fragmenting[6] metal wires to form sharp tips. Mechanically prepared tips usually suffer from poor reproducibility, lack of tip symmetry, large cone angle, and multiple tip formation. For samples with rough surfaces, such tips will produce nonrepresentative images of the surface, obviating the need for tips with well-defined geometry.

Physicochemical processes can be used to produce tips with well-defined shapes by controlling the processing parameters. Techniques include electrochemical polishing,[7] ion milling,[8,9] vapor deposition,[10] and electron beam deposition (EBD).[11,12] Historically, electrochemical polishing was the earliest technique for sharpening metal tips to very small radii,[13] and continues to be extensively used for making STM tips. A variety of methods, such as dc, ac, or pulsed voltage polishing, as well as combinations of these, by downward or upward (reverse) immersion of the metal wire into an appropriate electrolyte[4,7,14–35] have been reported. Electrochemically prepared tips are generally prepared by the dc drop-off method, since the shape produced, i.e., a hyperboloid, is desirable for STM images.[16] During dc electropolishing, thinning occurs at the electrolyte/air interface. The portion of the wire submerged in the solution ''drops off'' when its weight exceeds the strength of the wire in the reduced or necked region.[16]

Attempts at controlling relevant polishing parameters to improve reproducibility have been made. These include cutoff time, immersion depth, voltage, wave shape, phase angle, and frequency.[16,28] Automated processes have been developed,[16,28,29,36] with 100 nm radii tips being produced in some instances.[29] Optical microscopes[7] have also been used to monitor the process, as well as electrolyte dilution after neck-in has begun.[7] The aim of these innovations is to minimize cut-off response time.

Additional sharpening can be accomplished by localized polishing, which is designed to minimize the region of wire in contact with the electrolyte. Examples include the floating layer technique[20,37] and the loop technique.[38] Other techniques such as zone electropolishing[39] were designed to control the near-apex region aspect ratio or to make a desired tip geometry after the initial tip had already been made. Ultrasharp tips have also been fabricated by Fotino[4,14] using upward polishing as a second step for tip fabrication.

It is well known that W tips prepared by electropolishing are usually covered by a very thin layer of oxide (WO_3). The presence of surface oxide adversely affects STM image quality, manifesting as noise. Attempts to remove the oxide layer have been made using, for example, ion milling[8,9,40] with argon ions directed at the tip surface, annealing with electron bombardment at 1800 K,[41] or simply applying a wet chemical treatment to dissolve the oxide.[42] An electronic phase control unit has also been designed to control the second stage of electropolishing to make oxide free tips.[30]

Details of the above techniques can be found in the cited references and a number of review articles.[4,7,43]

As has already been mentioned, both tip shape and sharpness are of central importance for interpretation of STM images. Most tips are examined by scanning electron microscopy (SEM) at modest magnifications.[5,7,16,17,19,20,23,24,29,31,32,35,41,42,44–48] Recently, however, ultrasharp tip geometries have been characterized by high resolution transmission electron microscopy (TEM) at high magnifications. Examples of tips that have been examined include polished and ion milled W tips with radii of 10 to

200 nm[40] and 3 nm,[9] upward polished W tips with 1 nm minitips,[4,14] two-step polished tips with radii of 20 nm,[30] EBD tips with radii of 20 nm,[11] and Au-coated W tips with 20 nm gold clusters.[49]

A detailed study of the relationship between the tip geometry, true sample surface, and STM image is still lacking. Most STM papers either only give tip preparation and characterization information or present images from tips with unknown geometry.[50] Others present images of graphite surfaces [highly oriented pyrolytic graphite (HOPG)],[19,45–47,51,52] using atomic resolution of graphite to determine the tip quality.

Tips before and after scanning of platinum samples in ambient air have also been investigated by TEM to study tip deformation during scanning.[40] However, no supporting STM images were provided. Electropolished tips tested on Au samples were reported by Nicolaides *et al.*[17] using W tips and by Gorbunov, Wolf, and Edelmann[35] using Ag tips. More detailed studies were carried out by Fried, Wang, and Hipps,[49] using both electropolished W tips and Au-coated W tips, which had been characterized by TEM, on both smoother Au/C surfaces and rougher CuTCNQ surfaces.

Theoretical calculations aimed at determining the true surface structure from images distorted by finite-size tips have been done by several groups.[53–56] Keller[53] has reported that the local curvature of the sample surface is the sum of the tip curvature and the distorted STM image surface curvature. However, because the actual shape of the tips used to create the images was unknown, a parabolic or spherical shaped tip was assumed, and the tip radius was determined by comparing STM images with SEM images. A detailed relationship between well-characterized tips, known sample surfaces, and STM images is thus needed.

The purpose of this article is to fabricate STM tips from W by electrochemical polishing and a combination of electrochemical polishing and ion milling. Fabrication parameters are optimized in an effort to produce the sharpest, most reproducible tips. STM images of Au films on Si substrates, obtained using these tips, are then compared with TEM images and atomic force microscopy (AFM) images of the same films.

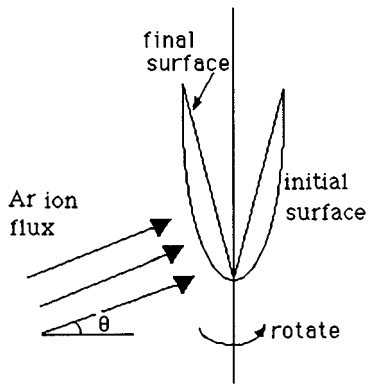

FIG. 1. Schematic illustration of ion milling process.

II. EXPERIMENT

The dc downward polishing method, similar to the process described in Ref. 16, was selected as the first stage for tip fabrication. Tungsten tips were prepared by placing several millimeters of the lower end of a polycrystalline W wire (0.5 mm in diameter) into an aqueous NaOH solution (2 or 3 M) and applying a positive dc voltage to the wire, making W the anode. The counterelectrode (or cathode) was stainless steel. The overall electrode reactions are given below:[16]

$$\text{cathode: } 6H_2O+6e^-\rightarrow 3H_2(g)+6(OH)^-,$$

$$\text{anode: } W(s)+8(OH)^-\rightarrow WO_4^{2-}+4H_2O+6e^-,$$

$$\text{overall: } W(s)+2OH^-+2H_2O\rightarrow WO_4^{2-}+3H_2\ (g)$$

$$(E^0=-1.43\ \text{V}).$$

To obtain macroscopically reproducible tip shapes, a micrometer assembly was used to accurately control the length

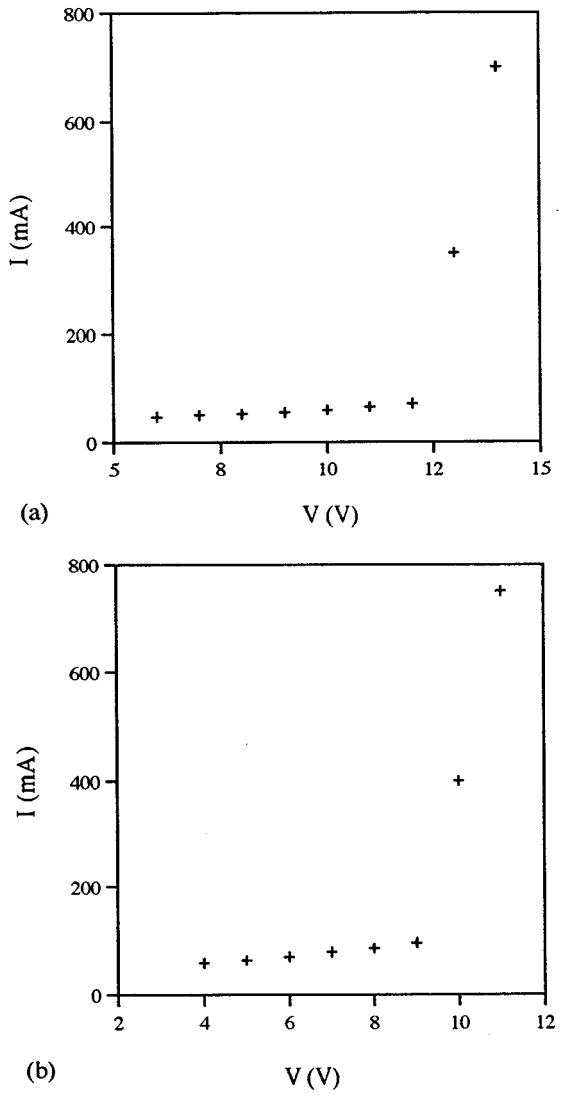

FIG. 2. Current (I) vs voltage (V) curves for electrochemical processing of W wire with an immersion depth of 2 mm. (a) 2 M NaOH solution; (b) 3 M NaOH solution.

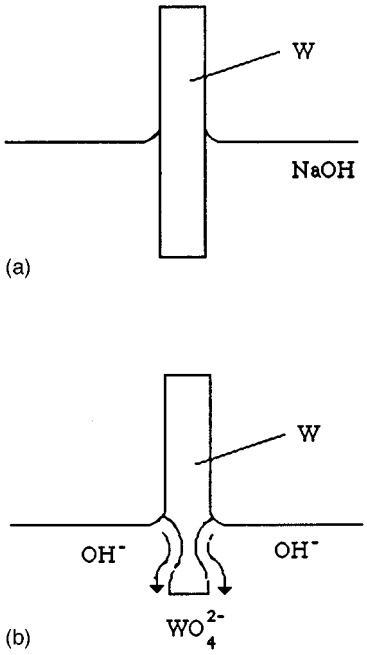

FIG. 3. Schematic showing the shape of the solution–air–W interfaces (Ref. 16).

of wire immersed in the solution. The electrochemical process was carefully monitored and stopped by turning off the voltage when the submerged portion of the wire dropped off. The tip was then immediately withdrawn and washed in two separate water baths for about 7 s each.

A Gatan ion mill (model No. 600 CTMP), which is commonly used for TEM sample preparation, was employed (at room temperature) for the second stage of tip fabrication. Tips were mounted on a tip holder vertically with the tip pointing downward and rotating at 2 rpm in a flux of 4.5 kV Ar ions. A single ion gun was employed using a current density of ≈ 1 mA/cm^2 and an incident angle of 30°. This arrangement is shown schematically in Fig. 1.

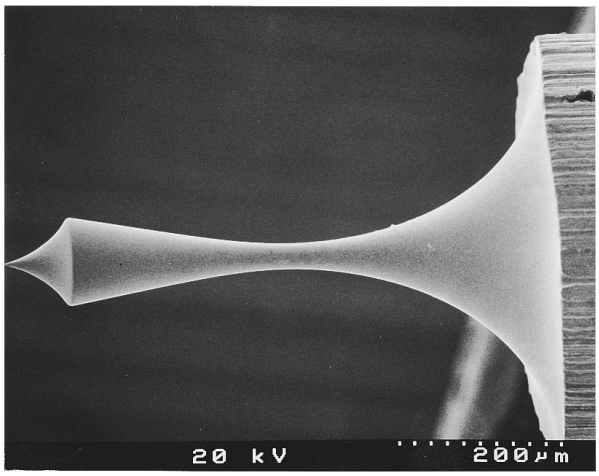

FIG. 4. SEM secondary electron (SE) image of W tip showing double necked regions. This is due to changing surface tension effects during processing.

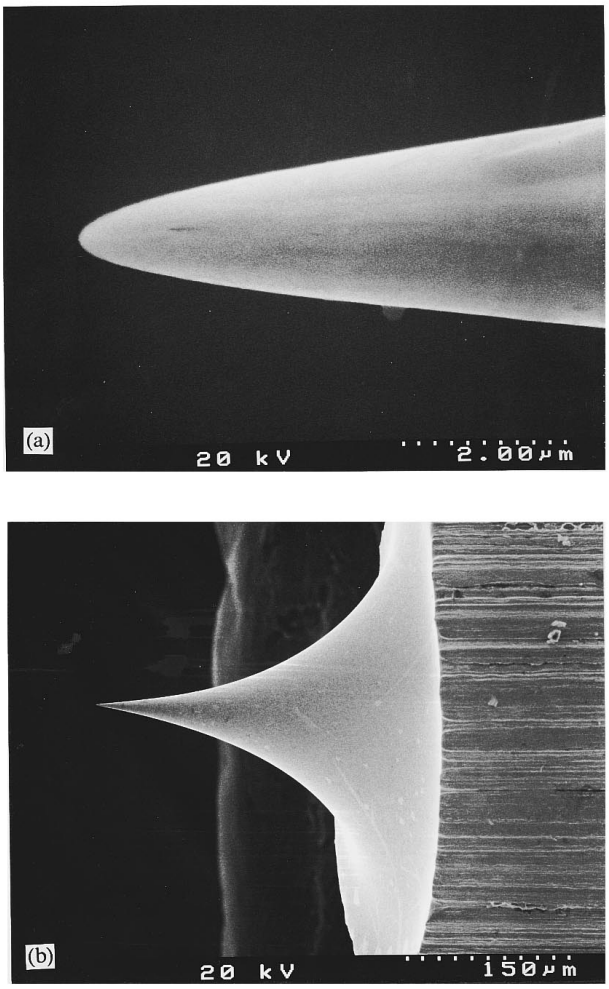

FIG. 5. SEM SE images of electropolished W tips. (a) High magnification image showing the radius of the tip; (b) low magnification showing the shape of the tip.

Electropolished tips and ion milled tips were examined before and after STM imaging using a Philips EM300 TEM operated at an accelerating voltage of 100 kV. The TEM images of tips presented here are all shadow images. SEM images of the tips were also obtained from a Hitachi S-2700 SEM operating at 20 kV and a working distance of 8–12 mm.

TABLE I. Relationship among the immersion depth d of W wire, the initial current $I1$ and the end current $I2$ just before dropoff.

	d (mm)	$I1$ (mA)	$I2$ (mA)
2 M NaOH, 11 V	1	30	20
2 M NaOH, 11 V	2	40–50	30
2 M NaOH, 11 V	3	60–70	40
3 M NaOH, 9 V	1	50–60	30
3 M NaOH, 9 V	1.5	70–80	40
3 M NaOH, 9 V	2	100–110	50
3 M NaOH, 9 V	3	120–160	80–90

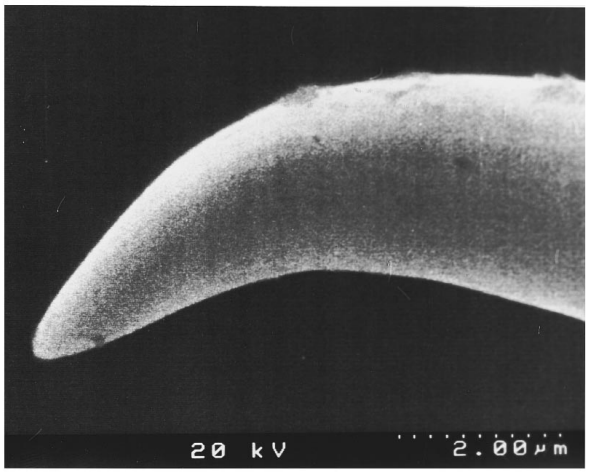

FIG. 6. SEM SE image of W tip processed with a 3 mm immersion depth.

STM images were obtained from a modified Burleigh Instructional STM operated in air and at room temperature. All images were taken in the constant current mode. The tip was biased at −50 mV relative to the sample with a tunneling current of 2 nA.

AFM images were obtained using a Topometrix TMX 2000 Discoverer scanning probe microscope (SPM) operated in the AFM mode. The force between the tip and sample was set at 0.08 nN, with a scanning speed of 4–8 Hz. EBD tips grown on Si_3N_4 pyramidal tips were used for imaging. The STM and AFM images shown in this article have not been processed, except for leveling.

Gold thin films deposited on ⟨100⟩ oriented Si substrates (doped to a level of 10^{15} cm^{-3}) were used for both STM and AFM imaging. The Au was deposited by electron beam evaporation in the form of circular contacts, approximately 10 nm thick and 2.5 mm in diameter. The grain size and thickness of the gold thin film were examined from plan view and cross section samples using a Hitachi H7000 TEM operating at an accelerating voltage of 120 kV. The STM and AFM images of the Au thin film were taken seven days after deposition.

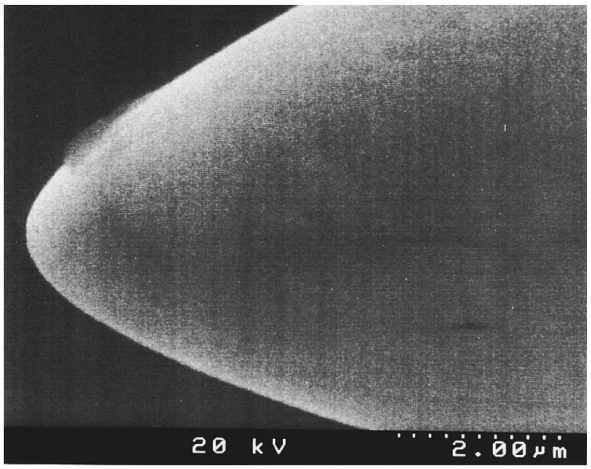

FIG. 7. SEM SE image of a W tip, showing the blunting effects of delay to cutoff.

TABLE II. Summary of electropolishing results.

Solution concentration	Voltage (V)	Total time (min)	Immersion depth (mm)	Results
2 M NaOH	11	12–14	1	Tips sharp
2 M NaOH	11	12–14	2	Tips sharp
2 M NaOH	11	12–14	3	Half of the tips bent
3 M NaOH	9	7–8	1	Tips a little broadened
3 M NaOH	9	7–8	1.5	Tips sharp
3 M NaOH	9	7–8	2	Tips sharp
3 M NaOH	9	7–8	3	Half of the tips bent

More than 50 fabricated tips were characterized by SEM and TEM. Once a reproducible procedure was developed, an additional 50 tips were fabricated for imaging tests.

III. RESULTS AND DISCUSSION

A. Tip preparation and characterization

The electrochemical process is comprised of etching, polishing or pitting, which depend on the current–voltage ($I-V$) relationship. Etching and pitting remove material at different rates locally producing surfaces with rough topography, and depend on factors such as crystallographic orientation, composition, and microstructure. Polishing tends to be insensitive to the above factors, removing material more rapidly from protrusions, producing a smoother surface. Since polycrystalline W was used to fabricate tips, the polishing regime was selected to produce well-defined tip surfaces. Typical $I-V$ curves are shown in Fig. 2 for 2 and 3 M NaOH solutions, for a wire immersion depth of 2 mm. Taking into account both polishing time and solution stability as discussed below, 11 and 9 V were selected as the polishing conditions for 2 and 3 M NaOH solutions, respectively.

When W wire is dipped into a NaOH solution, surface tension effects between the solution and wire control the interface shape (Fig. 3). On application of a positive voltage to the wire, the W will be oxidized to WO_4^{2-}, which goes into solution. A sheath of descending WO_4^{2-} around the lower part of the W wire shields it from further NaOH attack.[16] Thus, the reaction occurs mainly near the liquid surface, resulting in a necked-in effect. Parameters, such as voltage, solution concentration, and immersion depth, will affect the distribution of WO_4^{2-} and OH^- in the electrolyte and will change the interface shape, affecting the tip shape and sharpness. For this reason, the solution has to be maintained as mechanically stable as possible throughout the process.

A higher dc polishing voltage will reduce the processing time, thereby minimizing the effect of external vibrations. On the other hand, additional oxygen bubbles form from water or OH^- at the anode as a consequence of the higher voltage. Although the number of bubbles is insignificant rela-

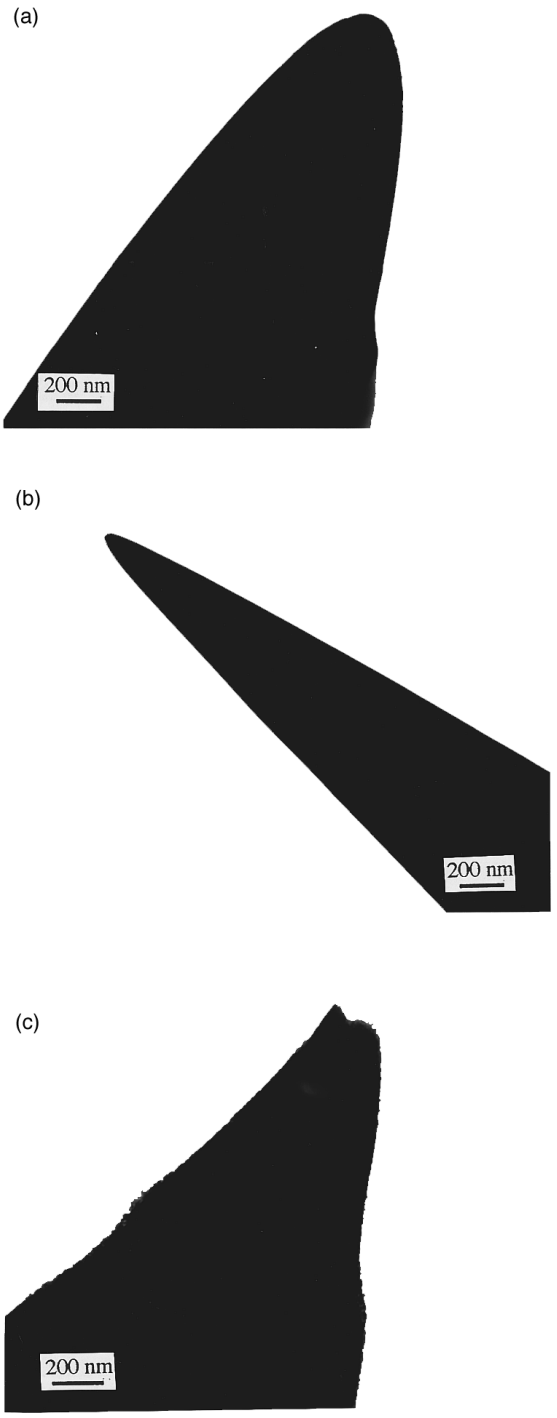

FIG. 8. TEM images of W tips prepared by a combination of electropolishing and ion milling. (a) Tip after electropolishing and prior to ion milling; (b) after ion milling for 40 min; (c) after ion milling for 3 h.

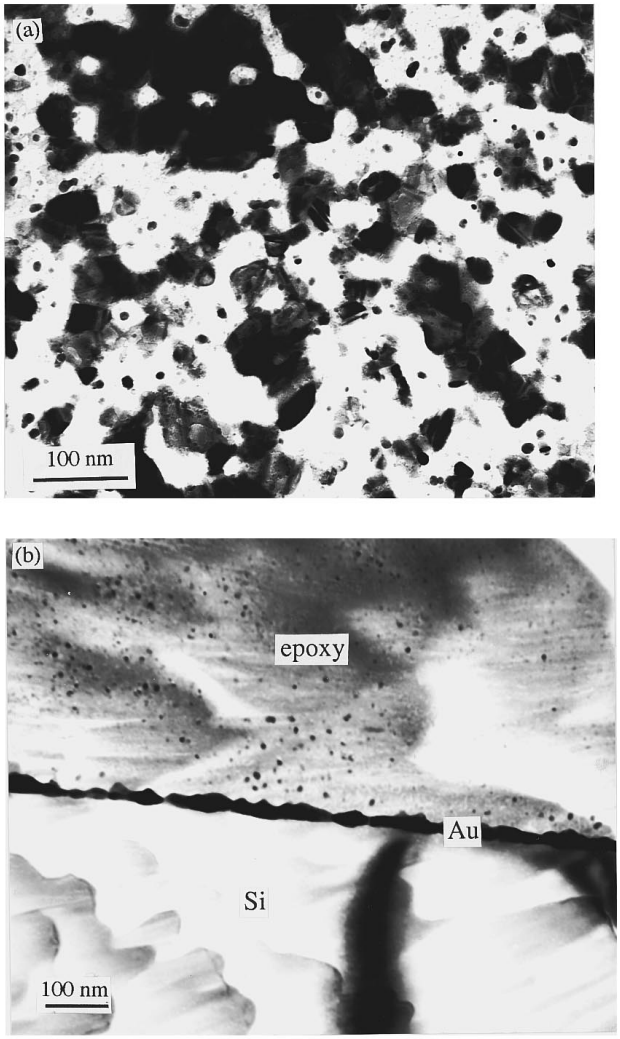

FIG. 9. TEM bright field images of Au film on ⟨100⟩ oriented Si. (a) Plan view image; (b) cross section image.

tive to ac polishing, bubbles can disturb the stability, particularly for fresh solutions, so that maintenance of the distribution of WO_4^{2-} and OH^- is not easy. The surface level always drops a little due to the neck-in effect, with a second neck-in region forming beneath (Fig. 4). Studies of voltage effects show that for 2 and 3 M NaOH solutions, voltages of 10–11 V and 8–9 V, respectively, will produce good tips. Voltages below 9 V for the 2 M solution and below 7 V for the 3 M solution will result in much longer processing times (more than 30 min), reducing stability, and increase the likelihood of poorly defined tips.

Electropolished tips exhibited nearly exponential shapes (Fig. 5), due to the slow decrease in current before the lower portion of the wire dropped off. Microscopically, maintaining a higher current means the concentration of OH^- at the W–liquid interface is higher, producing additional WO_4^{2-}. The effects of initial current (I_1) and final current before drop-off (I_2) are shown in Table I. The initial current I_1 increases as the length of the W wire in contact with the solution increases; however, tip shape does not change. Sharp tips can be reproducibly fabricated when the current is maintained at I_1 for at least half the process time, before it slowly decreases to I_2, prior to drop-off.

The effect of immersion depth has also been studied. Tips with an immersion depth of 3 mm in both 2 and 3 M solutions had, in addition to a macroscopic exponential shape, bent points (Fig. 6). It appears that too much of the wire is

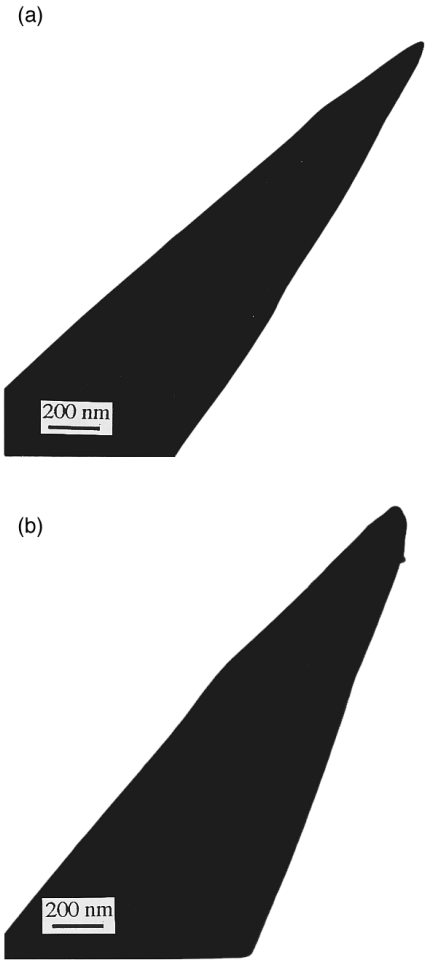

FIG. 10. TEM images of an ion milled tip (a) before and (b) after STM imaging of Au films.

submerged in this case leading to, according to Nicolaides *et al.*,[17] recoil or plastic flow when the tip is formed.

Another important factor in making sharp tips is the response time to shut off the voltage after drop-off, i.e., cut-off time. A delay of only 1 s can result in a broadened tip with a large cone angle (Fig. 7).

Table II summarizes the electropolishing results. The total processing time for a 2M NaOH solution at 11 V is 12–14 min, which produces tips with a radius of curvature of 200–250 nm with a cone angle of 25–35° at an immersion depth of 1–2 mm. Similar tips were obtained with 3 M NaOH solutions at 9 V and an immersion depth of 1.5–2 mm, after a total processing time of 7–8 min. Tip reproducibility was better than 90%.

Biegelsen and co-workers[8,9] have reported that ion milling is useful for removing the thin oxide layer which invariably forms during electrochemical polishing and reducing the tip radius. Although our ion milling process (Fig. 1) is different from theirs, the results are quite similar. Parameters such as voltage and current density affect thinning time, while incident angle affects the cone angle. Too small an incident angle will result in a larger tip cone angle. The optimum time for ion milling appears to be 30–40 min. TEM images of tips before and after ion milling are shown in Fig. 8, for two different ion milling times. For an ion milling time of 40 min, the tip radius is reduced from 250 to 20 nm and the cone angle is reduced from 35° to 25° [Figs. 8(a) and 8(b)]. For longer milling times, blunter tips or even multiple tips can form [Fig. 8(c)], which has been reported previously.[8] Multiple tip formation is due to the polycrystalline nature of W and selective thinning at W grain boundaries.[8]

B. STM on Au/Si(100)

In order to investigate the effect of tip geometry on STM images, information on both the sample and tip are necessary. A plan view section of the Au film on Si was made for TEM imaging [Fig. 9(a)]. The Au grain size could be easily measured and was determined to be 20–50 nm. A TEM cross section of the same sample [Fig. 9(b)] shows that the Au film is continuous but very much nonuniform, with a thickness varying from 8–33 nm.

Figure 10 shows TEM images of an ion milled W tip

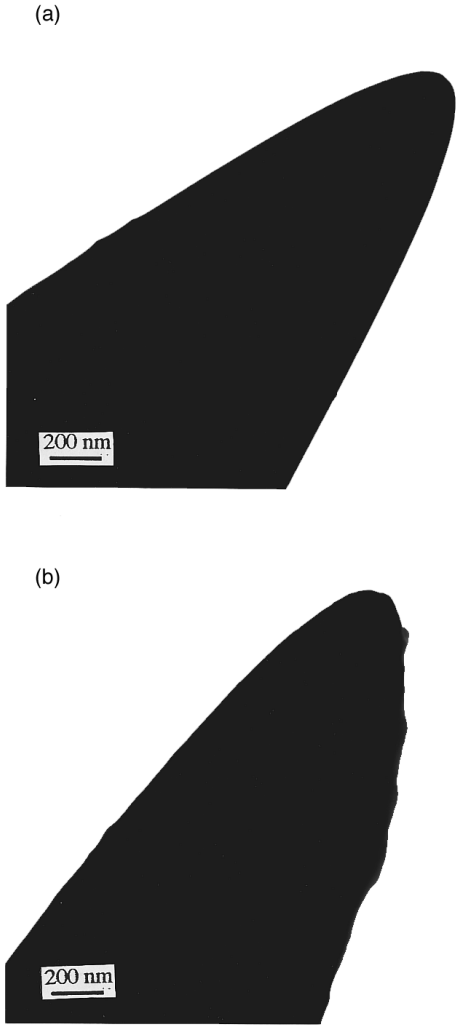

FIG. 11. TEM images of electropolished W tips (a) before and (b) after STM imaging of Au films.

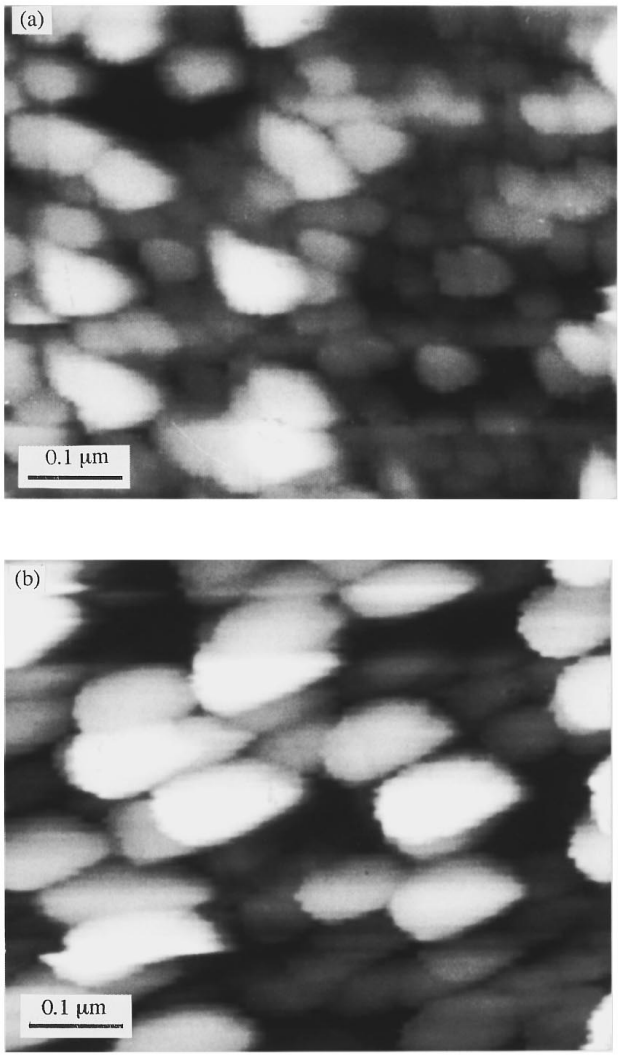

FIG. 12. STM images of Au films on ⟨100⟩ Si. (a) Image scanned with ion milled tip in Fig. 10. (b) Image scanned with electropolished tip in Fig. 11.

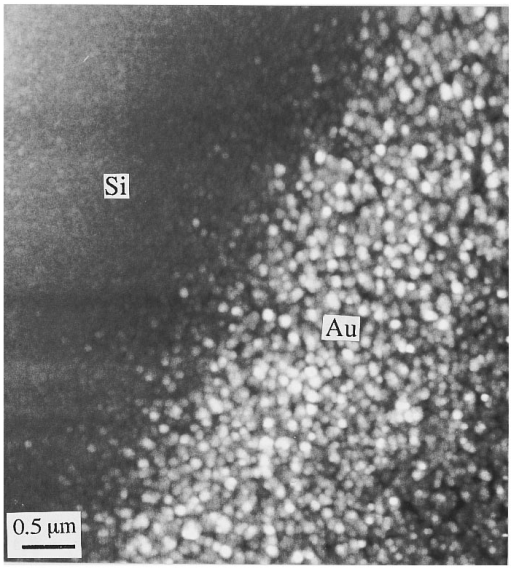

FIG. 13. AFM image scanned across edge of the Au film on ⟨100⟩ Si.

before and after STM imaging of the Au film. The tip radius was originally 20 nm with a cone angle of ≈23°. After scanning the tip is broadened and contaminated. TEM images of an electropolished W tip before and after scanning of the same sample are shown in Fig. 11. The tip radius is about an order of magnitude larger than the ion milled tip (200 versus 20 nm) and the cone angle is ≈35°. Again, after scanning the tip is contaminated and slightly deformed at the end. STM images obtained with the two tips are shown in Fig. 12. The apparent grain size for the ion milled tip is 40–90 nm [Fig. 12(a)] with a typical peak-to-peak roughness of 25 nm. The apparent grain size for the electropolished tip [Fig. 12(b)] is larger, i.e., 90–160 nm, although the peak-to-peak value remains similar (22 nm).

The STM results were also compared with AFM images, taken with EBD tips, of the same Au film (Fig. 13). The EBD tips had similar tip radii to the ion milled STM tips, but with higher aspect ratios. The apparent grain size from the AFM images is 30–90 nm with a typical peak-to-peak roughness of 23 nm. A line scan from the AFM (Fig. 13) showed that the Au film was ≈13 nm thick, which is within the range determined by TEM. The TEM, STM, and AFM results are summarized in Table III for comparison purposes.

According to Keller[53] the reconstructed true surface grain radius is equal to the STM image grain radius minus the tip radius (or plus the tip radius in the case of a hole). When the tip radius is smaller than or equal to the grain size, as for the

TABLE III. Comparison of Au grain size and thickness variation using various imaging techniques.

	Au grain size (nm)	Thickness variation (nm)	Peak-to-peak roughness (nm)	Tip radius (nm)	Tip cone angle (deg)
TEM	20–50	8–33	⋯	⋯	⋯
STM (ion milled tip)	40–90	⋯	25	20	23
STM (electropolished tip)	90–160	⋯	22	200	35
AFM (EBD tip)	30–90	13	23	20	10

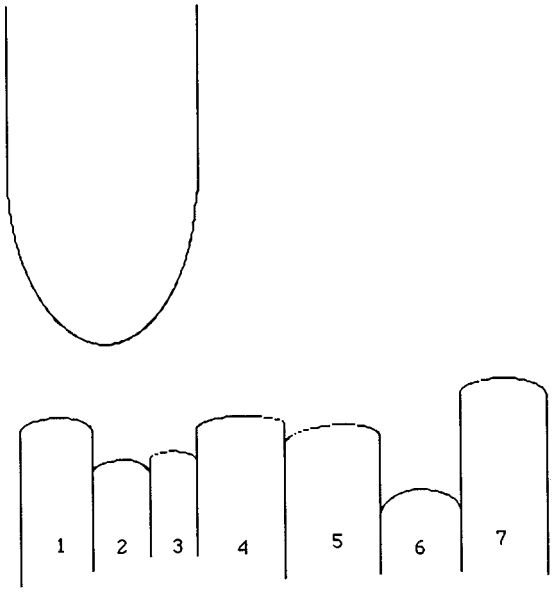

FIG. 14. Schematic showing the effect of a broad tip on imaging of polycrystalline films with a grain size smaller than the tip radius.

case of ion milled tips in the STM or EBD tips in AFM, the true grain radius is roughly within the range of the STM or AFM grain radius minus the tip radius (here, half of the grain size is used instead of the curvature of the Au grain). However, for the case where the tip radius is much larger than the grain size (electropolished tips), although Au grains can be resolved, the grain size resulting from these tips does not fit the reconstructed theoretical calculation. The grain size is doubled compared to the grain size resulting from sharper tips. In addition, the broadened tips may not protrude between the grains. Figure 14 schematically illustrates this effect. Grains 1, 4, 5, and 7 in the figure can be resolved by the tip, although the grain size in the image will be significantly larger than the actual size. Grains 2 and 3 may be resolved as a single grain, while grain 6 shows up as a hole. These effects can be seen in the STM images by comparing Figs. 12(a) and 12(b).

Finally, the tips after scanning under different conditions were examined by TEM (Fig. 15). An ion milled W tip, after scanning ten images of an Au/Si(100) sample, seven days after deposition, is shown in Fig. 15(a). The tip is bent with-

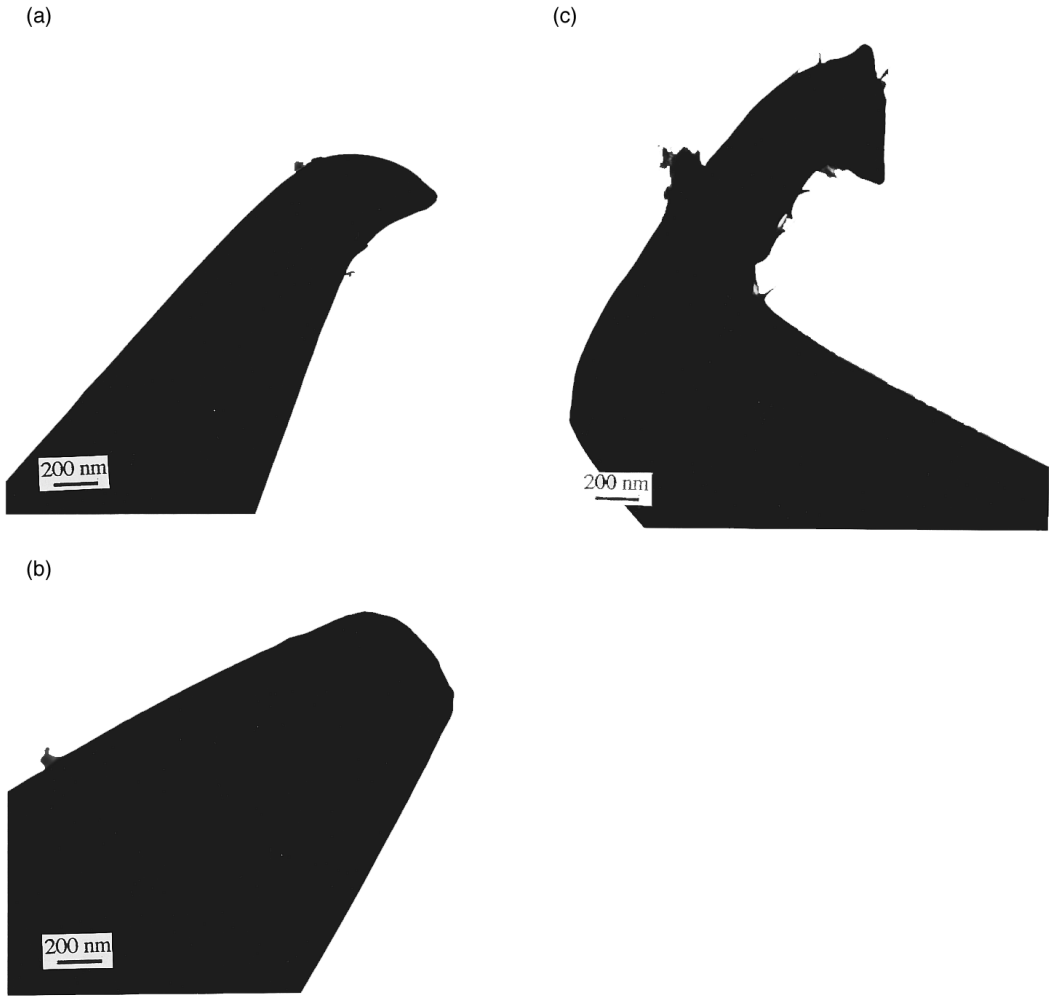

FIG. 15. TEM images of STM tips. (a) Ion milled W tip after scanning ten samples. (b) Electropolished W tip after crashing into sample. (c) Ion milled W tip after crashing into sample.

out apparently crashing into the sample. Garnaes *et al.*[40] have attributed tip bending to the presence of an oxide layer on the surface. However, we have not observed bending in electropolished tips, only in ion milled tips, where the oxide layer has been removed. The electropolished tips do flatten severely after crashing in a sample [Fig. 15(b)], but were too thick to bend. Ion milled tips bend severely after sample crashing [Fig. 15(c)]. Ion milled tips do not bend after multiple scans (more than 20 images) on smoother surfaces, such as deposited Au films on InP (images not shown here). The Au films, in this case, have a typical peak-to-peak roughness of 3–10 nm in STM images. A very small amount of deformation at the very end of the tip occurs, similar to that shown in Fig. 10(b). In the conventional view of STM, the tip–sample separation is assumed to be sufficiently large (0.6–1 nm) to allow only weak coupling between their electronic states. As the tip–sample distance decreases (0.2–0.6 nm), the potential barrier is lowered, inducing attractive forces. In the case of rougher surfaces, the feedback electronics is unable to keep up with sudden topographic changes, so the distance between the tip and the sample decreases momentarily. If the force exceeds the yield strength of the tip, irreversible tip deformation occurs. Thus the tip bending is not related to surface oxide in this case, but is due to the small tip radius, the rough topography of the sample surfaces, and the response of the feedback electronics. Reducing the scan rate may minimize the tip bending effect; however, the scan rate was experimentally determined to give the best quality image.

Electropolished tips tend to last much longer than ion milled tips. A possible explanation for this is that the tip radius of the ion milled tips is too small to withstand prolonged scanning without bending.

IV. SUMMARY

By carefully controlling the parameters, dc downward electrochemical polishing can produce initial tips with radii of the order of 200–250 nm. Subsequent ion milling can substantially reduce the tip radius to ≈20 nm. The two types of tips were used for STM imaging of Au films on ⟨100⟩ oriented Si and compared with TEM and AFM images. Apparent grain sizes appear to agree with theoretical calculations of finite-size tip distortion done by Keller.[53]

ACKNOWLEDGMENTS

This work was supported by a grant from the Natural Sciences and Engineering Research Council (NSERC) of Canada. The authors wish to thank Dr. Randy Mikula of CANMET for access to their AFM.

[1]G. Binnig, H. Rohrer, Ch. Gerber, and E. Weibel, Phys. Rev. Lett. **49**, 57 (1982).
[2]G. Binnig, H. Rohrer, Ch. Gerber, and E. Weibel, Appl. Phys. Lett. **40**, 178 (1982).
[3]G. Binnig, H. Rohrer, Ch. Gerber, and E. Weibel, Phys. Rev. Lett. **50**, 120 (1983).
[4]M. Fotino, Rev. Sci. Instrum. **64**, 159 (1993).
[5]W. E. Packard, Y. Liang, N. Dai, J. D. Dow, R. Nicolaides, R. C. Jaklevic, and W. J. Kaiser, J. Microsc. **152**, 715 (1988).
[6]A. J. Melmed, R. D. Shull, C. K. Chiang and H. A. Fowler, Science **239**, 176 (1988).
[7]A. J. Melmed, J. Vac. Sci. Technol. B **9**, 601 (1991).
[8]D. K. Biegelsen, F. A. Ponce, and J. C. Tramontana, and S. M. Koch, Appl. Phys. Lett. **50**, 696 (1987).
[9]D. K. Biegelsen, F. A. Ponce, and J. C. Tramontana, Appl. Phys. Lett. **54**, 1223 (1989).
[10]A. J. Melmed, J. Chem. Phys. **38**, 1444 (1963).
[11]Y. Akama, E. Nishimura, A. Sakai, and H. Murakami, J. Vac. Sci. Technol. A **8**, 429 (1990).
[12]B. Hubner, H. W. P. Koops, H. Pagnia, N. Sotnik, J. Urban, and M. Weber, Ultramicroscopy **42–44**, 1519 (1992).
[13]E. W. Muller, Z. Phys. **131**, 136 (1951).
[14]M. Fotino, Appl. Phys. Lett. **60**, 2935 (1992).
[15]P. J. Bryant, H. S. Kim, Y. C. Zheng, and R. Yang, Rev. Sci. Instrum. **58**, 1115 (1987).
[16]J. P. Ibe *et al.*, J. Vac. Sci. Technol. A **8**, 3570 (1990).
[17]R. Nicolaides *et al.*, J. Vac. Sci. Technol. A **6**, 445 (1988).
[18]J. Méndez, M. Luna, and A. M. Baró, Surf. Sci. **226**, 294 (1992).
[19]M. J. Heben, M. M. Dovek, N. S. Lewis, R. M. Penner, and C. F. Quate, J. Microsc. **152**, 651 (1988).
[20]H. Lemke, T. Göddenhenrich, H. P. Bochem, U. Hartmann, and C. Heiden, Rev. Sci. Instrum. **61**, 2538 (1990).
[21]J. E. Demuth, R. J. Hamers, R. M. Tromp, and M. E. Welland, IBM J. Res. Dev. **30**, 396 (1986).
[22]J. E. Demuth, R. J. Hamers, R. M. Tromp, and M. E. Welland, J. Vac. Sci. Technol. A **4**, 1320 (1986).
[23]I. H. Musselman, P. A. Peterson, and P. E. Ressell, Precision Eng. **12**, 3 (1990).
[24]I. H. Musselman and P. E. Russell, J. Vac. Sci. Technol. A **8**, 3558 (1990).
[25]R. Erlandsson, G. M. McClelland, C. M. Mate, and S. Chiang, J. Vac. Sci. Technol. A **6**, 266 (1988).
[26]G. Reiss, J. Vancea, H. Wittmann, J. Zweck, and H. Hoffmann, J. Appl. Phys. **67**, 1156 (1990).
[27]R. J. Colton, S. M. Baker, R. J. Driscoll, M. G. Youngquist, J. D. Baldeschwieler, and W. J. Kaiser, J. Vac. Sci. Technol. A **6**, 349 (1988).
[28]H. Morikawa and K. Goto, Rev. Sci. Instrum. **59**, 2195 (1988).
[29]R. Fainchtein and P. R. Zarriello, Ultramicroscopy **42–44**, 1533 (1992).
[30]J. P. Song, N. H. Pryds, K. Glejbol, K. A. Morch, A. R. Thölén, and L. N. Christensen, Rev. Sci. Instrum. **64**, 900 (1993).
[31]L. A. Nagahara, T. Thundat, and S. M. Lindsay, Rev. Sci. Instrum. **60**, 3128 (1989).
[32]M. Gehrtz, H. Strecker, and H. Grimm, J. Vac. Sci. Technol. A **6**, 432 (1988).
[33]T. Göddenhenrich, U. Hartmann, M. Anders, and C. Heiden, J. Microsc. **152**, 527 (1988).
[34]T. Tiedje, J. Varon, H. Deckman, and J. Stokes, J. Vac. Sci. Technol. A **6**, 372 (1988).
[35]A. A. Gorbunov, B. Wolf, and J. Edelmann, Rev. Sci. Instrum. **64**, 2393 (1993).
[36]R. J. Morgan, J. Sci. Instrum. **44**, 808 (1967).
[37]J. E. Fasth, B. Loberg, and H. Nordén, J. Sci. Instrum. **44**, 1044 (1967).
[38]Th. Michely, K. H. Besocke, and M. Teske, J. Microsc. **152**, 77 (1988).
[39]A. J. Melmed and J. J. Carroll, J. Vac. Sci. Technol. A **2**, 1388 (1984).
[40]J. Garnaes, F. Kragh, K. A. Morch, and A. R. Thölén, J. Vac. Sci. Technol. A **8**, 441 (1990).
[41]A. Cricenti, E. Paparazzo, M. A. Scarselli, L. Moretto, and S. Selci, Rev. Sci. Instrum. **65**, 1558 (1994).
[42]L. A. Hockett and S. E. Creager, Rev. Sci. Instrum. **64**, 263 (1993).
[43]D. A. Bonnell, *Scanning Tunneling Microscopy and Spectroscopy*, (VCH, New York, 1993), p. 155.
[44]S. Chiang and R. J. Wilson, IBM J. Res. Dev. **30**, 515 (1986).
[45]R. J. Colton, S. M. Baker, J. D. Baldeschwieler, and W. J. Kaiser, Appl. Phys. Lett. **51**, 305 (1987).
[46]M. Yata, M. Ozaki, S. Sakata, T. Yamada, A. Kohno, and M. Aono, Jpn. J. Appl. Phys. **28**, L885 (1989).
[47]M. J. Heben, M. M. Dovek, N. S. Lewis, R. M. Penner, and C. F. Quate, J. Microsc. **152**, 651 (1988).
[48]Vu Thien Binh, J. Microsc. **152**, 355 (1988).
[49]G. A. Fried, X. D. Wang, and K. W. Hipps, Rev. Sci. Instrum. **64**, 1495 (1993).

[50]A. Hammiche, R. P. Webb, and I. H. Wilson, Vacuum **45**, 569 (1994).
[51]C. A. Lang, J. K. H. Horber, T. W. Hansch, W. M. Heckl, and H. Mohwald, J. Vac. Sci. Technol. A **6**, 368 (1988).
[52]M. J. Heben, R. M. Penner, N. S. Lewis, M. M. Dovek, and C. F. Quate, Appl. Phys. Lett. **54**, 1421 (1989).
[53]D. Keller, Surf. Sci. **253**, 353 (1991).
[54]R. Chicon, M. Ortuno, and J. Abellan, Surf. Sci. **181**, 107 (1987).
[55]G. Reiss, F. Schneider, J. Vancea, and H. Hoffmann, Appl. Phys. Lett. **57**, 867 (1990).
[56]Ph. Niedermann and O. Fischer, J. Microsc. **152**, 93 (1988).